RPE | Radiation Physics & Engineering
An International Peer-Reviewed Journal
Published by K.N. Toosi University of Technology
http://rpe.kntu.ac.ir
Research Article

Radiation Physics and Engineering 2021; 2(2):21–28
https://doi.org/10.22034/rpe.2021.297939.1035

# Effect of ionic radius on Ti(IV), Zr(IV), and Hf(IV) adsorption by RB biomass

Saeed Kakaei, Elham Sattarzadeh Khameneh, Akbar Boveiri Monji*

*Radiation Application Research School, Nuclear Science & Technology Research Institute, P.O. Box 11365-3486, Tehran, Iran*

## HIGHLIGHTS

- High-affinity of RB biomass to sorption of zirconium and hafnium (>99%) due to their lower hydrated ionic radius.
- Interactions between hard-functional groups of RB biomass and hard cations of Ti(IV), Zr(IV), and Hf(IV).
- Widespread availability and low cost of proposed biosorbent.

## ABSTRACT

For the first time, sorption characteristics and mechanisms of group-4 elements were investigated and compared in extremely acidic solutions (4 M HCl) by rice bran (RB) biomass. Numerous instrumental strategies and hard-soft acid-base (HSAB) theory were applied to investigate the sorption features and mechanisms of Ti (IV), Zr (IV), and Hf (IV). The specific surface area of the raw biomass was 4.79 $m^2.g^{-1}$ as determined by Barrett-Emmet-Taller analyzer (BET). Deposition of planned metal ions on the biomass was determined through a scanning electron microscope (SEM) with energy-dispersive X-ray spectroscopy (EDS). The linkage of C=O, O-H, and N-H functional groups of biomass with metal ions became clear with Attenuated total reflection Fourier transform infrared (ATR-FTIR) spectrum analysis. The role of C=O functional group of ammonium oxalate/ammonium carbonate in metal ions desorption was confirmed by elution experiment. The experiments showed that the high-affinity of rubidium to sorption of zirconium and hafnium (>99%) was owing to their lower hydrated ionic radius. From all the results obtained, exhausting-hard interactions and electrostatic complexation mechanism were diagnosed between hard-functional groups of RB biomass and hard cations of Ti (IV), Zr (IV), and Hf (IV).

## KEYWORDS

Agricultural byproduct
Bio separation
Chemical interaction
Hard cations
Tetravalent metal

## HISTORY

Received: 02 August 2021
Revised: 07 September 2021
Accepted: 16 September 2021
Published: Spring 2021

## 1 Introduction

The group-4 elements lying within the d-block of the periodic table contain elements of titanium (Ti), zirconium (Zr), hafnium, (Hf), and rutherfordium (Rf). Since very little is understood regarding rutherfordium as a synthetic element, the foremost of the studies are centered on titanium, zirconium, and hafnium (Wiberg et al., 2007). Nowadays within the trade, to method and reuse Ti (IV), Zr (IV), and Hf (IV) as tetravalent transition metals (TVTM), completely different acids with high concentrations are used unceasingly for digestion of metal-bearing precipitation obtained from the leaching process. Therefore, it might be a difficult task to separate metals because of their associated extremely acidic media (Nayl et al., 2009; Eskandari Nasab et al., 2011). Over the previous few decades, biosorption of components has attracted great attention within the process and reprocessing plants and waste management due to economic and operational reasons like low operative expenses, a minimum volume of chemical waste, and/or biological sludge besides the high efficiency in detoxifying terribly dilute effluent (Kratochvil and Volesky, 1998). The biosorption of metals on the biomass surface happens in the main as a results of either physical interaction involving London-Vander Waals forces, or by chemical interaction like ionic or covalent binding between the adsorbent and also the adsorbate. The results of studies have disclosed that biosorption mechanisms rely on the sort of functional groups on the biomass surface, the nature of metal, and also the characteristics of the matrix round the biosorbent species (Guo et al., 2012; Hanif et al., 2015; Rahman et al., 2021). Though many studies were done on TVTM biosorption, all of them were conducted in a very gently acidic environ-

*Corresponding author: abovairi@aeoi.org.ir

ment (pH vary 2-5) and nearly no research in powerfully acidic solutions has been tested nevertheless. Indeed, the previous analysis projects in the main focused on the environmental aspects (Yaghmaei et al., 2014; Hanif et al., 2015). Given the economic importance of TVTM extraction from extremely acidic leach liquors, selective sorption of Zr and Hf ions was investigated from 4 M hydrochloric acid solutions by Rb in our former studies (Boveiri Monji et al., 2008; Stevenson et al., 2012). The obtained results showed that RB biomass as an agro industrial byproduct had the potential to be applied as a good biosorbent on an industrial scale owing to economic and operational edges like convenience in massive quantities, low economic value, wonderful sorption potency even in extreme acidic wastewater (99.8% and 99.5% for zirconium and hafnium respectively), high sorption rates, and straightforward operational method (no would like for pretreatment, modification, and immobilization). Additionally, it absolutely was disclosed that biosorption of *hard cations with high oxidation state*, Zr (IV) and Hf (IV), was abundant on top of soft, border and *hard cations with low oxidation state*. In line with our earlier investigation (Kakaei, 2018, 2019; Kakaei et al., 2020a,b; Kakaei and Xu, 2013a,b; Daneshvar et al., 2020), the current research was applied to seek out the attainable mechanism and chemical nature of TVTM accumulation by RB biomass. The mechanism of metal-biomass interaction was elucidated by using many analytical techniques like ATR-FTIR spectroscopy, SEM analysis, energy dispersive X-ray spectroscopy (EDS), cations transport check, and desorption process.

## 2 Experimental sections

### *2.1 Reagents*

All reagents were of pro-analysis grade and purchased from Merck Company. The stock solutions of 1000 $\mu$g.mL$^{-1}$ Zr and Hf were prepared by dissolving the suitable amounts of $ZrOCl_2.8H_2O$ and $HfOCl_2.8H_2O$ in 1000 mL double distilled water that was slightly acidified. The stock resolution of 1000 $\mu$g.mL$^{-1}$ titanium was ready by dissolving the appropriate amounts of $Ti(Cl)_4$ in concentrated HCl, transferring it to 1000 mL volumetric flask, and so transportation it to volume with double distilled water. Operating resolutions were ready daily by dilution of the stock solution with the distilled water and concentrated hydrochloric acid. Reagents were of pro-analysis grade and purchased from Merck Company. The stock solutions of 1000 $\mu$g.mL$^{-1}$ zirconium and hafnium were prepared by dissolving the appropriate amounts of $ZrOCl_2.8H_2O$ and $HfOCl_2.8H_2O$ in 1000 mL double distilled water that was slightly acidified. The stock solution of 1000 $\mu$g.mL$^{-1}$ titanium was prepared by dissolving the appropriate amounts of $Ti(Cl)_4$ in concentrated HCl, transferring it to 1000 mL volumetric flask and then bringing to volume with double distilled water. Working solutions were prepared daily by dilution of the stock solution with the distilled water and concentrated hydrochloric acid.

### *2.2 Preparation of biosorbent*

RB biomass was collected from micro industry of rice processing in Mazandaran, Iran. The samples were rinsed three times with water and finally with distilled water once more and oven dried at 60 °C for 24 h. The dried biosorbent was sieved to the particle size of 250 to 350 $\mu$m.

### *2.3 Physical properties of biomass*

#### 2.3.1 Elemental analysis of raw biomass

Three samples of raw biomass were considered for elemental analysis experiment. 10 g of each sample was heated with muffle furnace for combustion to a temperature of 1000 °C within 7 h. The remaining ash was allowed to cool in the muffle furnace for 24 h to room temperature and then re-weighed. At last, the elements present in the ash obtained from raw biomass were determined by an Oxford ED 2000 x-ray fluorescence (XRF) analyzer.

#### 2.3.2 Surface area, pore volume and pore size analysis

The surface area, pore volume and total pore size distribution were measured by a Quantachrome NOVA 2000e BET analyzer.

### *2.4 Mechanism determination experiments*

#### 2.4.1 Cations transport test

In this experiment, 50 mL of 4 M HCl solution (blank1/b1) was put it contact with 200 mg (dry wt.) of raw biomass (metal-free biomass). After 15 minutes shaking at 150rpm, the filtrate was separated (f1). In the following experiments, 50 mL of Ti(IV) solution (blank2/b2), 50 mL of Zr(IV) solution (blank3/b3) and 50 mL of Hf(IV) solution (blank4/b4) that each of them contains 50 mg.L$^{-1}$ cations concentration and 4 M HCl, was separately contacted with 200 mg (dry wt.) of RB biomass. After 15 minutes shaking at 150 rpm, the filtrates (f2, f3, or f4 obtained from b2, b3, or b4 respectively) were separated from metal-loaded biomass by Whatman-42 ashless filter paper. The elemental contents of all blanks and filtrates quantitatively analyzed and compared with each other by a Perkin-Elmer Optima 7300 DV Inductively Coupled Plasma Optical Emission Spectrometer (ICP-OES). The sorption efficiency of TVTM, R%, was calculated by using the Eq. (1):

$$R(\%) = (C_o - C_e/C_o) \times 100 \quad (1)$$

where $C_o$ and $C_e$ are the initial and equilibrium concentrations (mg.L$^{-1}$) of analyte ions in solution, respectively. All experiments were conducted in triplicate to ensure more accurate sorption results.

#### 2.4.2 SEM and EDS spectroscopy

The metal-free and metal-loaded biomass were examined by SEM-EDS spectroscopy (ZEISS-SIGMA, VP-SEM-EDS). The SEM-EDS procedure at ×50,000 magnification

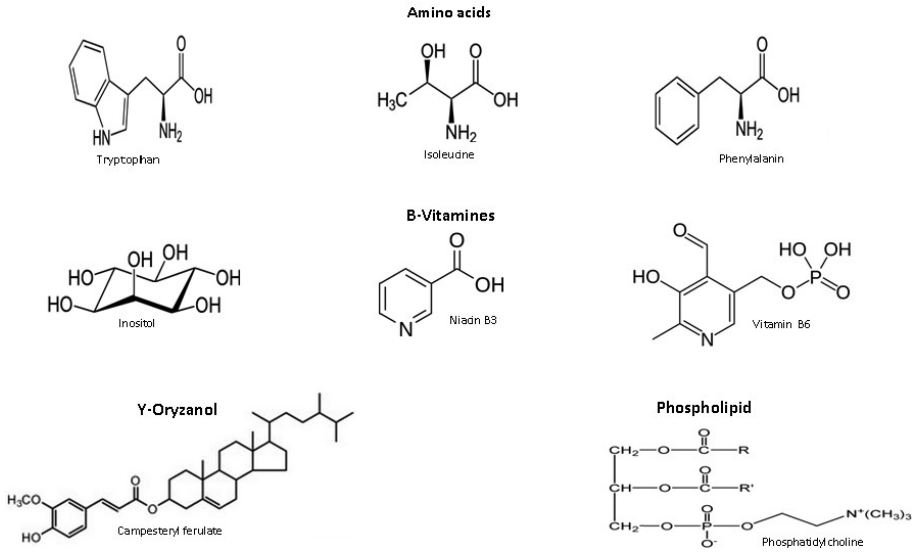


**Figure 1:** Some organic compounds in rice bran biomass.

with an accelerating voltage of 15 kV was applied to investigate the surface structures and elemental characteristics before and after biosorption process.

#### 2.4.3 ATR-FTIR spectroscopy

The organic functional groups of metal-free and metal-loaded biomass were analyzed using a Bruker Tensor 27 ATR-FTIR spectrometer. The infrared spectra were recorded in the range of 400 to 4000 $cm^{-1}$.

#### 2.4.4 Elution process

Batch desorption studies on metal-loaded biomass were conducted by various eluting agents such as NH4NO3, NH4SCN, (NH4)2SO4, $(NH_4)_2CO_3$ and $(NH_4)_2CO_4$ at concentrations from 0.1 to 1 M. After optimizing concentration of eluting agents, 0.5 M $NH_4NO_3$, 0.1 M $(NH_4)_2SO_4$, 1M $NH_4SCN$, 0.2 M $(NH_4)_2CO_3$ and 0.2 M $(NH_4)_23C_2O_4$ were used for trial. To desorb cations from the biomass surface, the filtered biomass was eluted with 10 mL of the eluting agents. Afterwards, the concentrations of the TVTM in eluent solution (The equilibrium concentration) were directly determined by ICP-OES. The amount of cations sorbed onto biomass (qsorp, $mg.g^{-1}$), the amount of cations desorbed into the eluent solution (qdes, $mg.g^{-1}$) and the percentage of desorbed cations (% desorption) were calculated by using the Eqs. (2), (3), and (4), respectively:

$$q_{sorp} = (C_o - C_e)V/m \quad (2)$$

$$q_{des} = C_{des}V/m \quad (3)$$

$$\%\ \text{desorption} = [q_{des}/q_{sorp}] \times 100 \quad (4)$$

where $m$ is sorbent weight in g, $V$ is the volume of the sample solution in L, and $C_{des}$ is metal concentration in the eluent in $mg.L^{-1}$.

## 3 Results and discussion

### *3.1 Physical properties and constituents of biomass*

#### 3.1.1 Mineral composition, specific surface area and total pore size of raw biomass

17.2%±2.34 ashes from burning 10 g raw biomass at 1000 °C were obtained. In other words, about 82.8% of the total weight of biomass contained volatile elements of oxygen, nitrogen and carbon which were removed from the biomass by burning. Thirteen elements as metal oxides were detected in the ash extracted from raw biomass by XRF method. The weight percent of elemental oxides in the analyzed sample followed the order $SiO_2$ (79.32)> $P_2O_5$ (10.27)> $K_2O$ (3.39)> MgO (2.09)> $Al_2O_3$ (1.74)> CaO (1.62)> $Na_2O$ (0.63)> $SO_3$ (0.35)> $Fe_2O_3$ (0.28)> MnO (0.07)> ZnO (0.06)> PbO (0.04)> $Cr_2O_3$ (0.02).

The specific surface area of the raw biomass was 4.79 $m^2.g^{-1}$ as determined by the BET method. Also, pore volume and pore size were 6.644 $cm^2.g^{-1}$ and 2.3 nm, respectively calculated by Barret-Joyner-Halenda (BJH) method.

#### 3.1.2 Biomolecules and functional groups on biomass cell walls

To better understand the effective interactions between biomass and metal ions, it is necessary to have accurate information about biomass cell structure. Rice bran is made up amino acids, cellulose, vitamins, phospholipids, flavonoids/polyphenols, phytosterols, carotenoids, oryzanols, tocopherols/tocotrienols, polysaccharids and enzymes. Some of the most important molecular structure was shown in Fig. 1. As can be seen, a variety of functional groups such as carboxyl, hydroxyl, phosphate, ether, aromatic, amide and amine could be found in the RB cell structure (Cicero and Derosa, 2005).

**Table 1:** Classification of binding groups of biomolecules based on HSAB theory.

| Binding group | HSAB classification | Ligand atom | Occurrence in selected biomolecules |
|---|---|---|---|
| Hydroxyl | Hard | O | PS, UA, SPS, AA |
| Carbonyl (ketone) | Hard | O | Peptide bond |
| Carboxyl | Hard | O | UA, AA |
| Sulfhydryl (thiol) | Soft | S | AA |
| Sulfonate | Hard | O | SPS |
| Thioether | Soft | S | AA |
| Amine | intermediate | N | Cto, AA |
| Secondary amine | intermediate | N | Cti, PG, Peptide bond |
| Amide | intermediate | N | AA |
| Imine | intermediate | N | AA |
| Imidazole | Soft | N | AA |
| Phosphate | Hard | O | PL |
| Phosphodiester | Hard | O | TA, LPS |

**Table 2:** Cations concentration change before and after biosorption.

| Element | Na(I) | K(I) | Ca(II) | Mg(II) | Zn(II) | Mn(II) | Pb(II) | Cr(III) | Al(III) | Fe(III) | Ti(IV) | Zr(IV) | Hf(IV) |
|---|---|---|---|---|---|---|---|---|---|---|---|---|---|
| b1 | 7.90 | 0.22 | 4.37 | 1.63 | 0.08 | 0.02 | 0.03 | 0.04 | 0.04 | 0.24 | - | - | - |
| f1 | 8.55 | 42.79 | 5.45 | 22.45 | 0.47 | 0.72 | 0.06 | 0.08 | 0.10 | 0.46 | - | - | - |
| Change[a] 1 | 0.65 | 42.57 | 1.08 | 20.82 | 0.39 | 0.7 | 0.03 | 0.04 | 0.06 | 0.22 | - | - | - |
| Total change[b] 1 | | | | | | | 66.56 | | | | | | |
| b2 | 9.18 | 0.41 | 3.83 | 1.73 | 0.05 | 0.07 | 0.01 | 0.09 | 0.14 | 0.14 | 52.63 | - | - |
| f2 | 11.03 | 42.31 | 5.14 | 22.97 | 0.29 | 0.42 | 0.15 | 0.17 | 0.29 | 0.51 | 11.57 | - | - |
| Change 2 | 1.85 | 41.90 | 1.31 | 21.24 | 0.24 | 0.35 | 0.14 | 0.08 | 0.15 | 0.37 | 41.06(78.0)[c] | - | - |
| Total change 2 | | | | | | | 67.63 | | | | | | |
| b3 | 7.46 | 0.53 | 5.42 | 0.87 | 0.09 | 0.05 | 0.02 | 0.04 | 0.06 | 0.27 | - | 48.30 | - |
| f3 | 8.02 | 45.54 | 6.27 | 24.81 | 0.27 | 0.59 | 0.10 | 0.11 | 0.31 | 0.61 | - | 0.15 | - |
| Change 3 | 0.56 | 45.01 | 0.85 | 23.94 | 0.18 | 0.54 | 0.08 | 0.07 | 0.25 | 0.34 | - | 48.17(99.7) | - |
| Total change 3 | | | | | | | 71.82 | | | | | | |
| b4 | 7.08 | 0.60 | 7.21 | 1.27 | 0.04 | 0.04 | 0.01 | 0.03 | 0.03 | 0.45 | - | - | 53.69 |
| f4 | 7.91 | 45.39 | 8.19 | 24.70 | 0.51 | 0.37 | 0.03 | 0.09 | 0.79 | 1.08 | - | - | 0.46 |
| Change 4 | 0.83 | 44.79 | 0.98 | 22.43 | 0.47 | 0.23 | 0.02 | 0.07 | 0.76 | 0.63 | - | - | 53.23(99.1) |
| Total change 4 | | | | | | | 71.21 | | | | | | |

a) Difference between ions concentration in f and b.
b) Sum of the change of cations concentration except hard cations.
c) Sorption efficiency percentage.

There is some evidence that confirm functional groups on biomass cell walls participate directly in binding certain cations (Wang and Chen, 2009). Table 1 represents the most representative functional groups and some of biomolecules in biomass, potentially involved in the sorption processes (Volesky, 2007).

### *3.2 Mechanism determination*

#### 3.2.1 Cations transport test

For a more detailed analysis of the biosorption mechanism, at first, cations transport test was performed in 4 M HCl without the presence of TVTM to recognize the role of hydrogen ions in sorption mechanism (test 1). Then, cations transport test was done in presence of 4 M HCl solutions containing TVTM (test 2, 3, and 4). As seen in Table 2, after contacting raw biomass with only 4 M HCl solution (b1), a large number of cations were released from the biomass to the solution (f1) which revealed ion exchange between hydrogen ions and the released cations were performed. Among them the changes of K (I) and Mg (II) ions concentrations were found to be greater than other cations. In test 2, during the process of TVTM biosorption from 4 M HCl solution (tests 2, 3, and 4), TVTM quantitatively were adsorbed onto the biomass. The change of Ti(IV), Zr(IV) and Hf(IV) ions concentration were represented in the *change 2*, *change 3*, and *change 4*, respectively. As can be observed the *total change 1* approximately equals to *the total change 2/3/4* which clearly indicates that hydrogen ions are the main agent of the cations released into the solution. In other words, the ion exchange mechanism could not be the main mechanism involved in sorbing TVTM by biomass.

#### 3.2.2 SEM images

The SEM technique was used to display surface morphology changes of the biomass before and after adsorbing TVTM. For further details of the surface morphology of raw RB, the images were taken from two distinctive areas of the biomass. As it can be seen, a whole surface with round-shape particles (Fig. 2-b) and a wrinkled surface

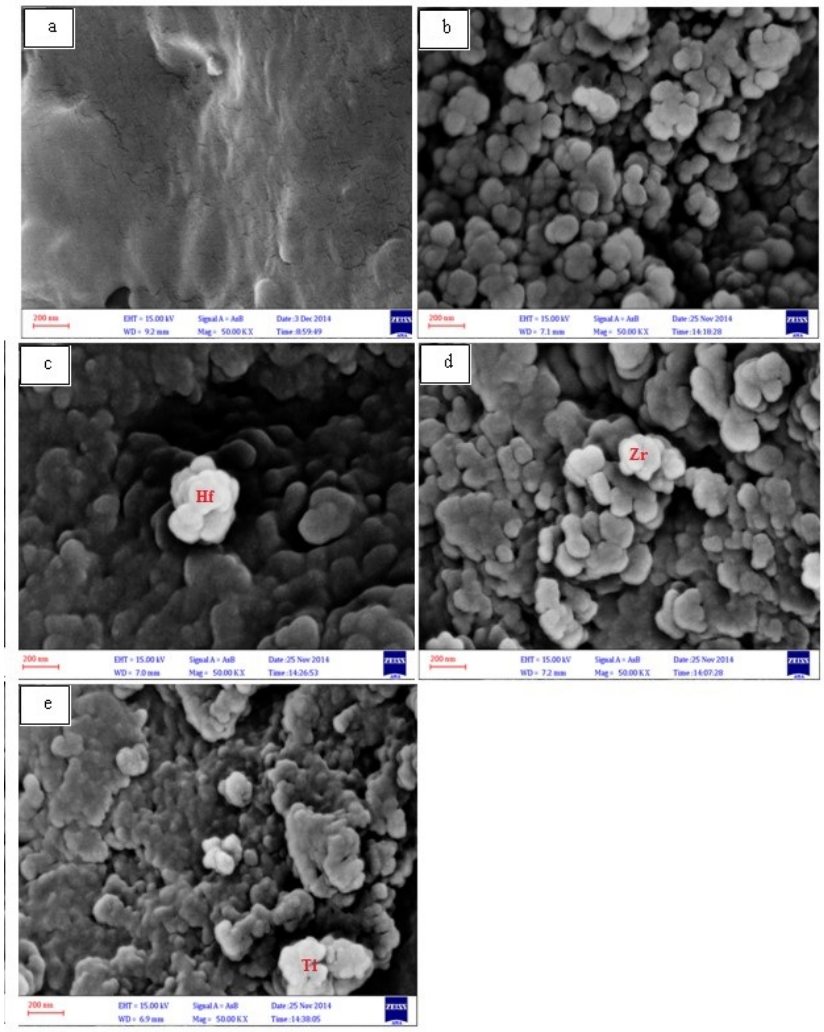


**Figure 2:** SEM images of metal-free RB (a and b), Hf-loaded RB (c), Zr-loaded RB (d), and Ti-loaded RB (e).

without particles (Fig. 2-a) were observed on the surface of biomass. Therefore, it can be concluded that TVTM are faced with completely uneven and irregular surface of biomass. The surface morphology of metal-loaded RB was greatly different from the native one. The granular aggregate deposition with brightness was clearly observed (Figs. 2-c, 2-d, and 2-e) on the SEM images of the metal-adsorbed samples.

### 3.2.3 EDS analysis

Further evidence of the metal ions adsorption onto RB biomass was achieved by EDS analysis. Figure 3 shows the EDS spectra of the metal-free and metal-loaded RB. Before the treatment, the EDS spectrum of biomass revealed the presence of C, N, O, P, Si, K, and Mg (spectrum 1). After treating with only 4 M HCl, K, and Mg peaks were disappeared this obviously exhibits that ion exchange mechanism is involved between K and Mg elements and hydrogen ions (Spectrum 2). After biosorption of TVTM from 4 M HCl solution, the EDS spectra of the precipitate clearly showed the presence of the adsorbed cations on the biomass (spectra 3, 4, and 5). Moreover, the peaks of C, N, O, P, and Si still existed on the cell surface after the metal ions treatment. The obtained findings of the EDS analysis correspond well with cation transport test and confirmed that except ion exchange, another mechanism was involved between TVTM and biomass which was discussed in the next sections.

### 3.2.4 ATR-FTIR analysis

ATR-FTIR spectroscopies of the biomass before (Fig. 4-a) and after TVTM biosorption (Fig. 4-b) were recorded to elucidate the functional groups involved in metal binding on RB biomass. Due to strong chemical interactions between cations and functional groups on the biomass, the following changes were clearly observed in Fig. 5 the peak intensities of metal loaded biomass at 3564 $cm^{-1}$ and 3300 $cm^{-1}$ clearly increased and decreased respectively, which is related to O-H stretching bond of carboxylic acids/phenols. The C=O peak of carboxylic acids/aldehydes/ketones at 1704 $cm^{-1}$ shifted to 1716 $cm^{-1}$ with increased intensity. Furthermore, the peak at 1650 $cm^{-1}$ which could be attributed to C=O stretching bond of amides shifted to 1641 $cm^{-1}$ with reduced in-

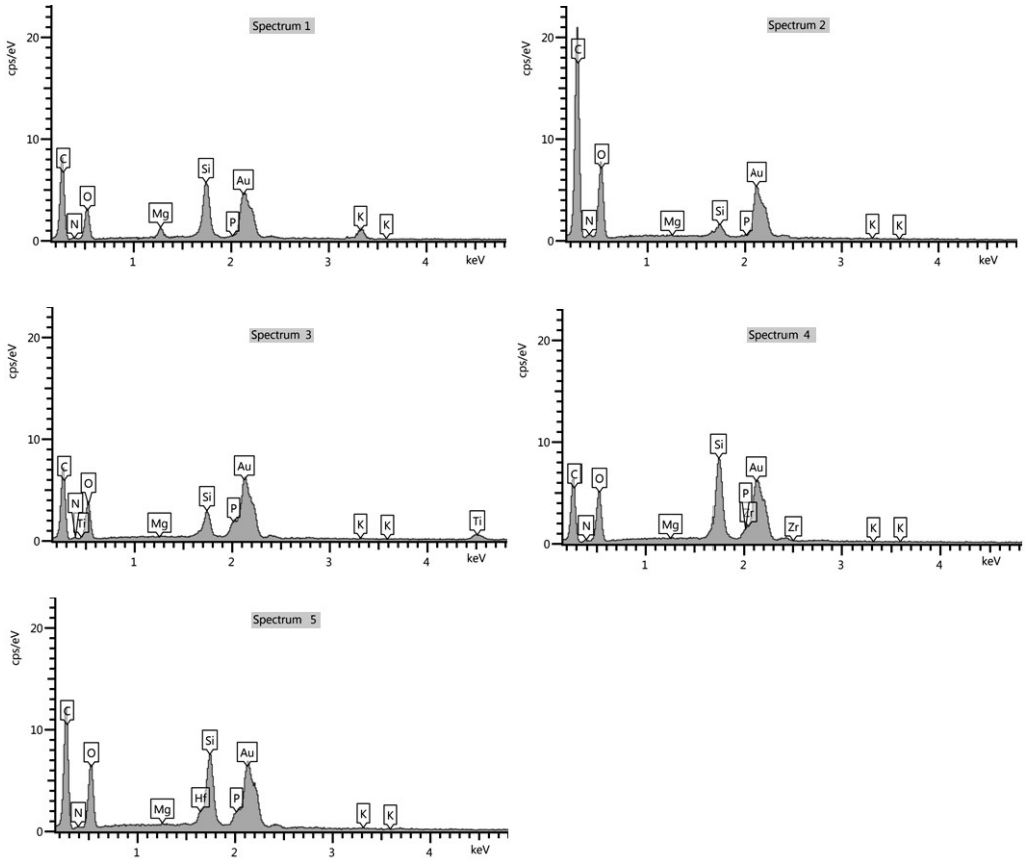


**Figure 3:** EDS spectra of metal-free RB (spectrum 1), H-loaded RB (spectrum 2), Ti-loaded RB (spectrum 3), Zr-loaded RB (spectrum 4), and Hf-loaded RB (spectrum 5).

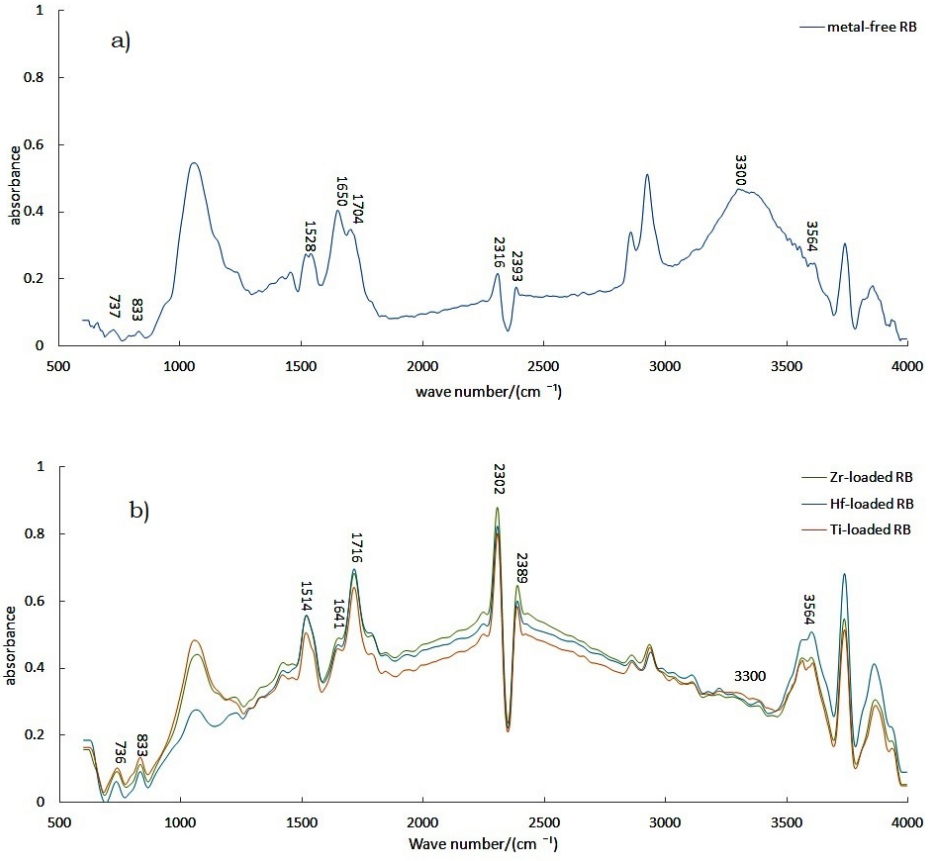


**Figure 4:** ATR-FTIR spectra of metal-free RB (a), and metal-loaded RB (b).

tensity. The shifted peak from 1528 $cm^{-1}$ to 1514 $cm^{-1}$ could be assigned to N-H bending bond of amide II band. The two peaks appeared at 737 $cm^{-1}$ and 833 $cm^{-1}$ for metal-loaded biomass may be relevant to C-H bending bond of aromatics. These results indicated that the functional groups such as C=O, O-, H, and N-H are mostly responsible for the binding of metal ions.

### 3.2.5 Elution behaviors of TVTM

In order to desorb analyte from the surface, cations exchangers are used more often and cations are exchanged with $H^+$, $NH_4^+$ or other cations derived from the ion exchange phase. Hence, in this trial, some cations exchangers containing $NH_4^+$ were compared to desorb TVTM from the biomass surface. As seen in Fig. 5, among various eluting agents, ammonium oxalate and carbonate were found to be successful in recovering TVTM from RB biomass due to strong interactions of functional group of C=O with cations. Titanium recovery was more than two other metal ions which show weaker interactions with RB functional groups. Also, TVTM ions were slightly desorbed with sulphate anion due to formation of anionic complex, [A (SO4)4]4-(aq).

### 3.2.6 HSAB theory

On the basis of HSAB theory, hard acids form stronger complexes with hard bases rather than soft bases. In general terms hard-hard interactions are predominantly electrostatic (ionic) whereas soft-soft interactions are predominantly covalent in nature (Pearson, 1963). Complex formation involves both covalent and electrostatic components whose relative contribution can be estimated by investigating how specific the binding is. When purely electrostatic attraction occurs, the binding strength should correlate with the charge density ($z^2/r_{hyd}$). Ions of the same charge $z$ and hydrated radius $r_{hyd}$ should therefore be bound with equal strength. Major deviations of the binding strength from the $z^2/r_{hyd}$ correlation indicate a tendency towards a covalent bond character (Naja and Volesky, 2011).

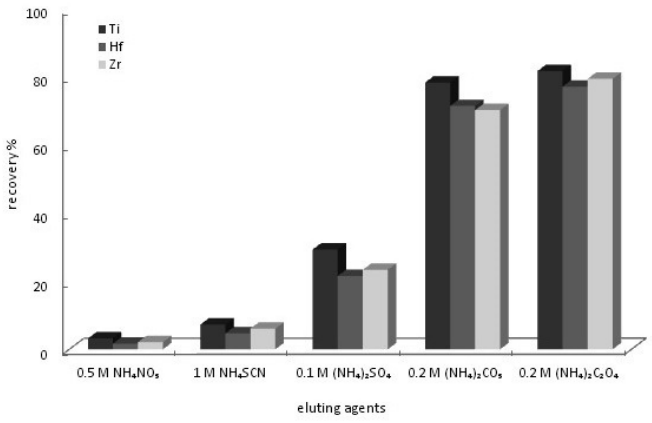


**Figure 5:** Effect of eluent type on the recovery of TVTM.

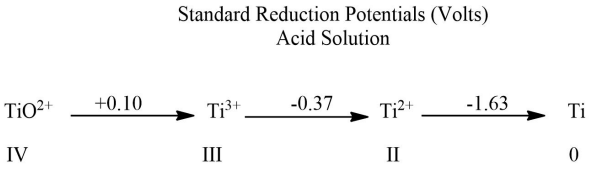


**Figure 6:** Standard reduction potentials of titanium.

Because of the lanthanide contraction of the elements in the fifth period, zirconium and hafnium have nearly identical ionic radii. This similarity results in nearly identical chemical behavior and in the formation of similar chemical compounds (Barrett, 2003). The only states of Zr and Hf in highly acidic aqueous solution are the +4 ions. Their reduction potential are -1.55 and -1.7 V respectively which imply that $Zr^{4+}$ and $Hf^{4+}$ ions are stable in the acidic environment (Chandra, 2006). $Ti^{4+}$ ions do not exist in solution due to high charge to radius ratio but oxo ions ($TiO^{2+}$/ titanyl) are formed instead. Titanium has oxidation states IV (most stable), III (reducing), and II (strongly reducing) (Shannon, 1976). The formal reduction potential of titanium in acidic aqueous solution is shown in Fig. 6.

Although the crystal ionic radius of Ti is smaller than Zr and Hf, the hydrated ionic radius of Ti is greater than that of Zr and Hf because Ti(IV) exists in the form of $TiO^{2+}$ while both Zr(IV) and Hf(IV) exist as $Zr^{4+}$ and $Hf^{4+}$ ions (Kielland, 1937; Yu, 1997). For cations of the same valence, the adsorption strength should be determined mainly by the hydrated radius of the ions (Stevenson et al., 2012). Therfore, though $TiO^{4+}$ like two other families, $Zr^{4+}$ and $Hf^{4+}$, is a hard cations with high oxidation state (tetravalent), it is considered a weaker hard cations due to higher hydrated ionic radius. As a result, as indicated in Table 2, sorption efficiency of $Zr^{4+}$ and $Hf^{4+}$ (>99%) is more than $TiO^{2+}$ (78%).

In general, knowledge of the biosorption mechanism is not easily obtained since we are not dealing with simple and clearly recognized chemical compounds. Biosorbents comprise different types of cells with highly complex structures whose various building blocks consist of a multitude of different molecules which in turn can display several binding sites (Stevenson et al., 2012). Nevertheless, due to the hard nature of Ti (IV), Zr (IV), and Hf (IV) and also the presence of hard-functional groups such as OH, CO, COOH, and COOR in the structure of RB biomolecules, the ionic complexation mechanism was recognized between RB biomass and hard cations with high oxidation state.

## 4 Conclusion

Cations transport test showed despite the existence of ion exchange interaction between biomass and TVTM, it only had a trivial contribution in the biosorption mechanism. ATR-FTIR spectroscopy and desorption technique clearly proved hard-hard interactions between TVTM and hard-functional groups. From all the results obtained, it can be deduced that the electrostatic complexation mechanism is predominant between RB functional groups and TVTM. It

seems that biomolecules such as amino acids, B-vitamins, phospholipids, and oryzanols containing hard-functional groups play a significant role in biosorption of TVTM.

## Acknowledgment

The authors gratefully acknowledge the support of the present work by Radiation Application Research School, Nuclear Science & Technology Research Institute, P.O. Box 11365-3486.

## References

Barrett, J. (2003). *Inorganic chemistry in aqueous solution*, volume 21. Royal Society of Chemistry.

Boveiri Monji, A., Javad Ahmadi, S., and Zolfonoun, E. (2008). Selective biosorption of zirconium and hafnium from acidic aqueous solutions by rice bran, wheat bran and platanus orientalis tree leaves. *Separation Science and Technology*, 43(3):597–608.

Chandra, S. (2006). *Comprehensive Inorganic Chemistry Vol. Ii*. New Age International.

Cicero, A. F. and Derosa, G. (2005). Rice bran and its main components: potential role in the management of coronary risk factors. *Current Topics in Nutraceutical Research*, 3(1):29–46.

Daneshvar, H., Shafaei, M., Manouchehri, F., et al. (2020). Influence of morphology and chemical processes on thermoluminescence response of irradiated nanostructured hydroxyapatite. *Journal of Luminescence*, 219:116906.

Eskandari Nasab, M., Milani, S., and Sam, A. (2011). Extractive separation of Th(IV), U(VI), Ti(IV), La(III) and Fe(III) from zarigan ore. *Journal of Radioanalytical and Nuclear Chemistry*, 288(3):677–683.

Guo, J., Zheng, X.-d., Chen, Q.-b., et al. (2012). Biosorption of Cd(II) from aqueous solution by pseudomonas plecoglossicida: kinetics and mechanism. *Current microbiology*, 65(4):350–355.

Hanif, A., Bhatti, H. N., and Hanif, M. A. (2015). Removal of zirconium from aqueous solution by Ganoderma lucidum: biosorption and bioremediation studies. *Desalination and Water Treatment*, 53(1):195–205.

Kakaei, S. (2018). PVP-and PEG-grafted Ni Doped Iron Oxide Nanoparticles for Biomedical Applications: Electrochemical Synthesis and Characterization.

Kakaei, S. (2019). Ethylenediaminetetraacetic Acid and Polyvinyl Chloride Grafted Zinc Cations doped Magnetite Nanoparticles for Biomedical Applications: Electrochemical Synthesis and Characterization.

Kakaei, S., Khameneh, E., Hosseini, M., et al. (2020a). A modified ionic liquid clay to remove heavy metals from water: investigating its catalytic activity. *International Journal of Environmental Science and Technology*, 17(4):2043–2058.

Kakaei, S., Khameneh, E. S., Rezazadeh, F., et al. (2020b). Heavy metal removing by modified bentonite and study of catalytic activity. *Journal of Molecular Structure*, 1199:126989.

Kakaei, S. and Xu, J. (2013a). Efficient synthesis of protected sulfonopeptides from N-protected 2-aminoalkyl xanthates and thioacetates. *Tetrahedron*, 69(43):9068–9075.

Kakaei, S. and Xu, J. (2013b). Synthesis of (2-alkylthiothiazolin-5-yl) methyl dodecanoates via tandem radical reaction. *Organic & biomolecular chemistry*, 11(33):5481–5490.

Kielland, J. (1937). Individual activity coefficients of ions in aqueous solutions. *Journal of the American Chemical Society*, 59(9):1675–1678.

Kratochvil, D. and Volesky, B. (1998). Advances in the biosorption of heavy metals. *Trends in biotechnology*, 16(7):291–300.

Naja, G. and Volesky, B. (2011). The mechanism of metal cation and anion biosorption. In *Microbial biosorption of metals*, pages 19–58. Springer.

Nayl, A., El-Nadi, Y., and Daoud, J. (2009). Extraction and separation of Zr(IV) and Hf(IV) from nitrate medium by some CYANEX extractants. *Separation science and Technology*, 44(12):2956–2970.

Pearson, R. G. (1963). Hard and soft acids and bases. *Journal of the American Chemical society*, 85(22):3533–3539.

Rahman, M., Wong, Z. J., Sarjadi, M. S., et al. (2021). Heavy metals removal from electroplating wastewater by waste fiber-based poly (amidoxime) ligand. *Water*, 13(9):1260.

Shannon, R. D. (1976). Revised effective ionic radii and systematic studies of interatomic distances in halides and chalcogenides. *Acta crystallographica section A: crystal physics, diffraction, theoretical and general crystallography*, 32(5):751–767.

Stevenson, L., Phillips, F., O'sullivan, K., et al. (2012). Wheat bran: its composition and benefits to health, a European perspective. *International journal of food sciences and nutrition*, 63(8):1001–1013.

Volesky, B. (2007). Biosorption and me. *Water research*, 41(18):4017–4029.

Wang, J. and Chen, C. (2009). Biosorbents for heavy metals removal and their future. *Biotechnology advances*, 27(2):195–226.

Wiberg, N., Wiberg, E., and Holleman, A. F. (2007). Lehrbuch der Anorganischen Chemie, 102. Aufl.

Yaghmaei, S., Roostaazad, R., Mohammad-Beigi, H., et al. (2014). Removal of zirconium from aqueous solution by Aspergillus niger. *Scientia Iranica*, 21(3):772–780.

Yu, TR, e. (1997). *Chemistry of variable charge soils*. Oxford University Press.